Journal of Hazardous Materials 416 (2021) 125788

Contents lists available at ScienceDirect

Journal of Hazardous Materials

journal homepage: www.elsevier.com/locate/jhazmat

Research Paper

Embryonic exposure to low concentrations of aflatoxin B1 triggers global transcriptomic changes, defective yolk lipid mobilization, abnormal gastrointestinal tract development and inflammation in zebrafish

Bence Ivanovics [a], Gyongyi Gazsi [a], Marta Reining [a], Izabella Berta [a], Szilard Poliska [b], Marta Toth [c], Apolka Domokos [b,d], Bela Nagy Jr [e], Adam Staszny [a], Matyas Cserhati [a], Eva Csosz [b], Attila Bacsi [c], Zsolt Csenki-Bakos [a], Andras Acs [a], Bela Urbanyi [a,*], Zsolt Czimmerer [b,*]

[a] Institute of Aquaculture and Environmental Safety, Hungarian University of Agriculture and Life Sciences, H-2100 Godollo, Hungary
[b] Department of Biochemistry and Molecular Biology, Faculty of Medicine, University of Debrecen, H-4032 Debrecen, Hungary
[c] Department of Immunology, Faculty of Medicine, University of Debrecen, H-4032 Debrecen, Hungary
[d] Molecular Cell and Immunobiology Doctoral School, Faculty of Medicine, University of Debrecen, H-4032, Debrecen, Hungary
[e] Department of Laboratory Medicine, Faculty of Medicine, University of Debrecen, H-4032 Debrecen, Hungary

ARTICLE INFO

Editor: Dr. S Nan

Keywords:
Aflatoxin B1
Embryonic toxicity
Zebrafish
Inflammation
Yolk lipid mobilization
L-arginine
Gastrointestinal tract development

ABSTRACT

Aflatoxin B1-contaminated feeds and foods induce various health problems in domesticated animals and humans, including tumor development and hepatotoxicity. Aflatoxin B1 also has embryotoxic effects in different livestock species and humans. However, it is difficult to distinguish between the indirect, maternally-mediated toxic effects and the direct embryotoxicity of aflatoxin B1 in mammals. In the present study, we investigated the aflatoxin B1-induced direct embryotoxic effects in a zebrafish embryo model system combining toxicological, transcriptomic, immunological, and biochemical approaches. Embryonic exposure to aflatoxin B1 induced significant changes at the transcriptome level resulting in elevated expression of inflammatory gene network and repression of lipid metabolism and gastrointestinal tract development-related gene sets. According to the gene expression changes, massive neutrophil granulocyte influx, elevated nitric oxide production, and yolk lipid accumulation were observed in the abdominal region of aflatoxin B1-exposed larvae. In parallel, aflatoxin B1-induced defective gastrointestinal tract development and reduced L-arginine level were found in our model system. Our results revealed the complex direct embryotoxic effects of aflatoxin B1, including inhibited lipid utilization, defective intestinal development, and inflammation.

1. Introduction

One of the most urgent challenges posed by the changing global environment is to manage the decrease in food and feed quality and quantity. As common contaminants of staple foods and feeds, mycotoxins may significantly contribute to these losses (Marroquín-Cardona et al., 2014). As the secondary metabolites of filamentous fungi, mycotoxins have various adverse effects on human and animal health (Hussein and Brasel, 2001). In the last decades, several predictive models have established aiming to forecast infection risk and mycotoxin contamination of crops during the pre-and postharvest periods (Battilani et al., 2012; Battilani and Leggieri, 2015; van der Fels-Klerx et al., 2010). However, climate change can extraordinarily influence the outcomes of these predictions. Relatively small changes in environmental conditions, including average temperature, precipitation pattern, and humidity, may promote fungal growth and mycotoxin production resulting in increased food and feed safety concerns (Marroquín-Cardona et al., 2014; Medina et al., 2014).

It has been well documented that aflatoxin B1 (AFB1) has the highest acute and chronic toxicity among mycotoxins, and the International Agency for Research on Cancer (IARC) classifies it as a Group-1 human carcinogen (IARC, 1993). AFB1 induces widespread harmful effects from hepatotoxicity (Lu et al., 2013; McGlynn et al., 2003) to impaired immunological (Jiang et al., 2005; Meissonnier et al., 2008; Reddy et al., 1987) and reproductive function (El-Azab et al., 2010; Supriya et al., 2014) in both humans and animals. The most endangered areas of AFB1

* Corresponding authors.
E-mail addresses: urbanyi.bela@szie.hu (B. Urbanyi), czimmerer.zsolt@med.unideb.hu (Z. Czimmerer).

https://doi.org/10.1016/j.jhazmat.2021.125788
Received 5 January 2021; Received in revised form 19 March 2021; Accepted 29 March 2021
Available online 2 April 2021

contamination are the tropical and subtropical regions (Gong et al., 2016; Wild et al., 1990). However, it is anticipated that the major AFB1 producer *Aspergillus flavus* and its toxic metabolites will become more frequent in the Mediterranean and temperate zones due to the increasing average temperature. The work of Battilani et al. (2016) draws attention to the potential emergence of AFB1 in maize even during cultivation in southern and certain central European countries under a + 2 °C climate change scenario. Similar predictions were made for the United States: the pre-harvest contamination of maize in the Corn Belt is expected to become an emerging food and feed safety issue in the near future (Mitchell et al., 2016; Yu et al., 2018).

In utero exposure to xenobiotics in mammals frequently results in developmental or metabolic alterations and leads to increased susceptibility to different diseases (Barr et al., 2007; Dufour-Rainfray et al., 2011; Selgrade et al., 2013). Furthermore, it should be emphasized that embryonic exposure to various environmental pollutants (e.g., heavy metals (Shirai et al., 2010), endocrine disruptors (Huang et al., 2014; Schönfelder et al., 2002) or pesticides (Ribas-Fitó et al., 2006)) can promote disease development or induce malformations at relatively low concentrations. It has been described that AFB1 can also cross the placental barrier and cause teratogenic and embryotoxic effects in mammals, therefore, maternal exposure may implies a serious health risk to the developing embryo (El-Nahla et al., 2013; Partanen et al., 2010; Wangikar et al., 2005). Furthermore, previous human studies demonstrated that elevated maternal aflatoxin-albumin adduct levels correlated with adverse birth outcomes (most commonly low birth weight) and postnatal growth faltering (Abdulrazzaq et al., 2002; Lauer et al., 2019; Smith et al., 2017; Turner et al., 2007). However, the biological consequences of embryonic exposition to AFB1 at low doses, especially in humans, are not completely understood.

The zebrafish (*Danio rerio*), as a promising vertebrate model organism, has appeared firstly in developmental and genetic studies and soon has become one of the most widely used in vivo models in many different research areas. The externally fertilized and transparent embryos can be easily monitored and manipulated, providing a useful in vivo system for toxicological investigations (Scholz et al., 2008). Zebrafish possess several conservative traits and functions compared to mammals and humans. The zebrafish genome-sequencing project has revealed that almost 70% of zebrafish genes have at least one human orthologue (Howe et al., 2013). Thus, developing zebrafish systems for modeling human diseases, including immunological and metabolic disorders, have become widely accepted (Anderson et al., 2011; Fang et al., 2014; Gomes and Mostowy, 2020; Iwanami, 2014; Meeker and Trede, 2008; Seth et al., 2013). In parallel, zebrafish is also a suitable model organism for the study of the role of xenobiotics in the evolvement of acute and chronic disorders (Lieschke and Currie, 2007; Scholz et al., 2008; Sun et al., 2020). AFB1-related diseases such as hepatocellular carcinoma and the toxin's metabolism have been investigated in zebrafish (Troxel et al., 1997; Wrighton et al., 2019). Exploring the effects of embryonic exposure to xenobiotics in mammals encounter limitations and generate ethical concerns. Besides, xenobiotics can affect the developing fetus directly and also indirectly through maternally-mediated harmful effects, making it challenging to explore the underlying mechanisms of embryotoxicity (Smith et al., 2017). The *ex utero* developing zebrafish embryos and larvae offer a cost-effective, non-mammalian vertebrate model system to reveal the direct toxic effects and the potential consequences of embryonic exposure to AFB1.

The present study aimed to investigate the direct adverse effects of embryonic exposure to AFB1 at relatively low, sublethal (<LC10) concentrations on zebrafish embryos and larvae integrating toxicological, transcriptomic, metabolomic, and immunological methodologies. Our strategy has led to the identification of various harmful effects of sublethal AFB1 exposure, including altered lipid transport and utilization, defective gastrointestinal tract development, elevated inflammation, and reduced L-arginine level.

2. Materials and methods

2.1. Ethics statement

Experiments were performed in accordance with the Hungarian Animal Welfare Law (XIV-I-001/2303–4/2012) and the European directive (2010/63/EU) on the protection of animals used for scientific purposes.

2.2. Chemicals

Aflatoxin B1; Oil red O (ORO); DAF-FM-DA (4-amino-5-methylamino-2′,7′-difluorofluorescein diacetate); Ringer tablets; Trypsin-EDTA solution; fetal bovine serum (FBS) and fluorescent microbeads (carboxylate-modified polystyrene, fluorescent red) were purchased from Sigma-Aldrich. Stock solution of AFB1 was prepared by dissolving the AFB1 powder in dimethyl sulfoxide (DMSO) to the concentration of 1 mg/mL and was stored at −24 °C.

2.3. Zebrafish maintenance and egg collection

The wild-type AB strain and the Tg(mpx:EGFP) transgenic line of zebrafish (Danio rerio) were maintained at the Department of Aquaculture (Szent Istvan University, Hungary) in a Tecniplast ZebTEC recirculation system (Tecniplast S.p.A., Italy) at 25.5 ± 0.5 °C, pH 7.0 ± 0.2, conductivity 550 ± 50 μS (system water) with 14 h/10 h light/dark cycles. Tg(mpx:EGFP) transgenic line (Mathias et al., 2006) were obtained from Karlsruhe Institute of Technology (KIT), Karlsruhe, Germany.

Before the spawning day, late in the afternoon males and females were placed separately in breeding tanks. On the morning after the onset of light the separation walls were removed allowing the fish to spawn. After the collection of eggs, about 2 h post fertilization, the embryos were sorted under a stereo microscope in order to select the normally developing ones and to synchronize their development.

2.4. Embryonic exposure to AFB1

The embryo toxicity test was conducted based on the OECD guideline 236 (2013). Test solutions were prepared by diluting stock solution (1 mg AFB1 / mL DMSO) with UV-disinfected, carbon filtered system water (parameters: 25.5 ± 0.5 °C, pH 7.0 ± 0.2, conductivity 550 ± 50 μS) as exposure medium. The embryos (n = 10 / replicate) were exposed individually to AFB1 at the concentrations of 0.03125, 0.0625, 0.125, 0.25 and 0.5 mg/L in 24-well plates (2 mL / well) from 4 to 120 h post fertilization (hpf) in two independent experiments with three replicates per group in each experiment. Mortality was monitored daily during the treatment period. In the control groups only one out of sixty embryo died during the treatment period (background mortality = 1.67%). 120-h lethal concentration values (LC1, LC10, LC50) were obtained by estimating the concentration-response relationship based on the lethal endpoints using OriginPro® (2018) software. Concentration-response relationship for estimation LC-values was performed according to the following equation: y = A1 + (A2-A1)/(1 + 10^((LOGx0-x)*p)), where: A1: bottom asymptote; A2: top asymptote; LOGx0: center; p: hill slope. Any further embryonic exposition was performed by using a sublethal, low concentration range (˂LC10) of AFB1. In these experiments, previously sorted embryos were exposed in goups to AFB1 at the concentrations of 0.025, 0.05, 0.075 and 0.1 mg/Lfrom 4 to 120 h post fertilization in polystyrene 100-mm Petri dishes containing 40 mL (20 embryo / Petri dish) or 45 mL (30 embryo / Petri dish) of test/control solutions DMSO was used as solvent control.

2.5. Evaluation of morphological alterations

The morphological changes of the larvae were assessed at the end of

the AFB1-exposure (120 hpf). The larvae were anesthetized with tricaine methane sulfonate (MS222, 168 mg/l, Matthews and Varga, 2012) positioned laterally and pictured under a stereo microscope (Leica M205 FA, Leica DFC 7000 T camera, Leica Application Suite X software, Leica Microsystems GmbH; Wetzlar, Germany). Total body length, swim bladder area and the length of the gut were measured by image analysis using ImageJ software (Schneider et al., 2012) (n = 3 replicates, n = 10 larvae per replicate).

2.6. Total RNA extraction and quantitative RT-PCR

Total RNAs from 30 pooled larvae per replicate (n = 5 replicates) were isolated by Trizol reagent. RNA quality and quantity were assessed by NanoDrop One (Thermo Fisher Scientific, Madison, USA) spectrophotometer. cDNA was synthesized from 1 μg of total RNA by using High Capacity cDNA Reverse Transcription kit (Applied Biosystems). Expression levels of reference and target genes were measured using 5x HOT FIREPol EvaGreen qPCR Supermix (Solis BioDyne) on a LightCycler 480 Instrument II (Roche). Nucleotide sequences of primers are shown in the Supplementary Table S1.

2.7. RNA sequencing and data analysis

To obtain global transcriptome data high throughput mRNA sequencing analysis was performed on Illumina sequencing platform. Total RNA sample quality was checked on Agilent BioAnalyzer using Eukaryotic Total RNA Nano Kit according to manufacturer's protocol. Samples with RNA integrity number (RIN) value > 7 were accepted for library preparation process. RNA-Seq libraries were prepared from total RNA using Ultra II RNA Sample Prep kit (New England BioLabs) according to the manufacturer's protocol. Briefly, poly-A RNAs were captured by oligo-dT conjugated magnetic beads then the mRNAs were eluted and fragmented at 94-Celsius degree. First strand cDNA was generated by random priming reverse transcription and after second strand synthesis step double stranded cDNA was generated. After repairing ends, A-tailing and adapter ligation steps adapter ligated fragments were amplified in enrichment PCR and finally sequencing libraries were generated. Sequencing run were executed on Illumina NextSeq500 instrument using single-end 75 cycles sequencing.

Raw sequencing data (fastq) was aligned to Danio rerio reference genome (version GRCz11) using HISAT2 algorithm and BAM files were generated. Downstream analysis was performed using StrandNGS software (www.strand-ngs.com). BAM files were imported into the software DESeq1 algorithm was used for normalization. To identify differentially expressed genes between treated and non-treated conditions Moderated T-test with Benjamini-Hochberg FDR for multiple testing correction was used. Significance was defined at corrected p value ⟨ 0.05. Raw sequencing data submitted to NCBI Sequence Read Archive (SRA) database (PRJNA684994).

2.8. Oil red O staining and assessment of lipid distribution

Oil red O (ORO) was used for staining neutral lipids in whole zebrafish larvae (Schlegel and Stainier, 2006). 10 larvae from each replicate (n = 2 replicates) were euthanized at 120 hpf by immersion in ice water, then washed in PBS and fixed in 4% paraformaldehyde at 4 °C for 6 h, washed again and stained with 0.1% filtered ORO in 60% isopropanol for 2 h. After incubation, the larvae were washed in PBS and gradually transferred into 95% glycerol. Bright field images from the lateral view of the larvae were taken under a Leica M205 FA stereo microscope. Lipid distribution was assessed by measuring optical density (OD) of the abdominal region (yolk and intestinal area) after OD calibration by Rodbard method (https://imagej.nih.gov/ij/docs/examples/calibration/) using ImageJ software.

2.9. Measurement of NO production

The NO production in zebrafish larvae was evaluated by using a fluorescent probe DAF FM DA. 120 hpf larvae from two independent experiments (n = 10 larvae per experiment) were transferred individually into 96-well plates containing 200 μL 5 μM DAF FM DA solution per well, and incubated in the dark at 25.5 °C for 1 h. After incubation, larvae were rinsed in system water, anesthetized in a solution of tricaine methane sulfonate (MS222, 168 mg/l), positioned laterally and imaged by using Leica M205 FA fluorescent microscope equipped with GFP2 long pass filter. Fluorescent intensity of the whole larva or the abdominal region alone were measured in greyscale using ImageJ software.

2.10. Investigation of arginine content

Nitric oxide production's substrate L-Arginine level was determined by UPLC spectrometry. Embryos were homogenized in 1% SDS-containing borate buffer (pH 9) with 19 G needles. The homogenate was centrifuged at 14000 rpm for 10 min using a benchtop Eppendorf centrifuge, and the supernatant was filtered through a 3 kDa filter (Pall) according to the manufacturer's instructions. The filtrate was dried in a speed-vac (Thermo Scientific), redissolved in 80 μL borate buffer and used for amino acid analysis. Derivatization was carried out with AccQ-Tag Ultra derivatization kit (Waters) and the samples were examined in duplicates on an H-class UPLC (Waters) according to the manufacturer's instructions. For data analysis the Empower software (Waters) was used.

2.11. Neutrophile number and distribution

To investigate the neutrophil granulocyte number and distribution, Tg(mpx:EGFP) transgenic zebrafish line was used. In Tg(mpx:EGFP) transgenic zebrafish line, the expression of enhanced green fluorescent protein (EGFP) transgen is driven by neutrophil granulocyte-specific myeloperoxidase (mpx) promoter (Renshaw et al., 2006). In order to measure the total number of neutrophils in whole larvae, fluorescence activated cell sorting (FACS) was conducted according to a previously published protocol (Oehlers et al., 2013). Briefly, 120 hpf Tg(mpx:EGFP) larvae from two independent experiments with three replicates per group (n = 15 larvae per replicate) were euthanized by submersion in ice water, then rinsed with Ringer solution and dissociated in 0.25% Trypsin-EDTA. Digestion was stopped by fetal bovine serum (FBS) and calcium chloride. Samples were centrifugated (400 g; 5 min), resuspended in 5% FBS/PBS, then filtered through 40 μm cell strainers. The frequency of GFP+ neutrophil granulocytes was determined by the NovoCyte Flow Cytometer (ACEA Biosciences). Neutrophile distribution in 120 hpf Tg(mpx:EGFP) larvae from three independent experiments (n = 10 larvae per experiment) was evaluated by visual observation and quantified by counting the neutrophils in the abdominal region. Images were taken from the lateral view of the larvae under a Leica M205 FA fluorescent microscope equipped with a GFP2 long pass filter.

2.12. Tail fin transection model

Tail fin transection were performed as previously described (Cheng et al., 2020), with minor modifications. 108 hpf Tg(mpx:EGFP) larvae from five independent experiments (n = 10 larvae per experiment) were anesthetized with tricaine methane sulfonate (MS222, 168 mg/l) and the tail fins of the larvae were transected along a straight line between the tip of the notochord and the caudal end of the fin. Neutrophil migration to the site of injury was monitored by imaging the caudal region of the larvae under a Leica M205 FA fluorescent microscope at 4 and 12 h post-injury. The number of neutrophils at the site of injury was counted using ImageJ software.

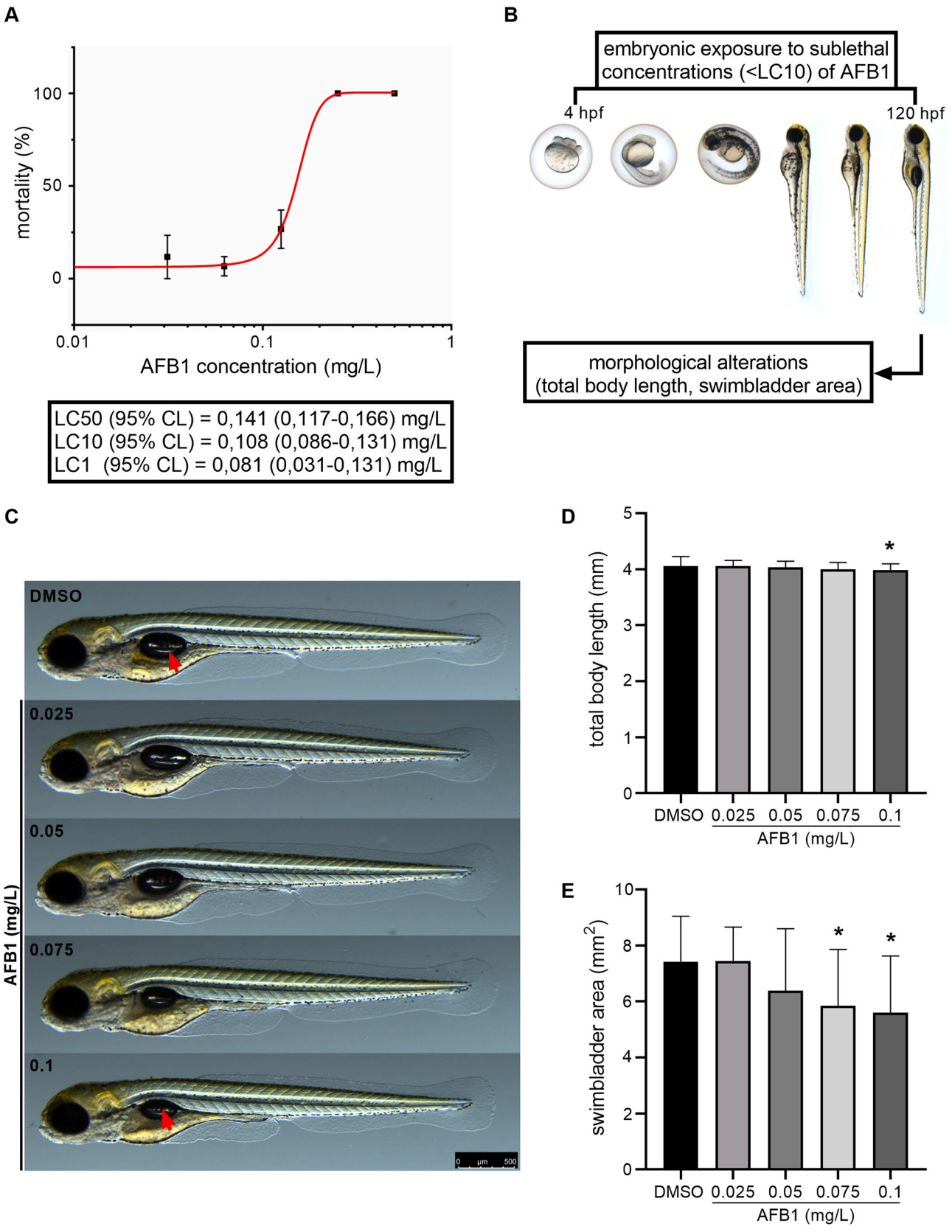

Fig. 1. Embryonic exposure to sub-lethal concentrations of AFB1 reduces total body length and swim bladder area. (A) Concentration-response relationship and the estimated LC% values for 120 h toxicity test of zebrafish embryos exposed to AFB1 (n = 6 replicates, n = 10 embryo per replicate). (B) Schematic representation of the applied experimental system. (C) Representative images of 120 hpf zebrafish larvae after embryonic, sub-lethal exposure to AFB1. Red arrows indicate swim bladder. Scale bar = 500 µm. The graphs showing (D) total body length and (E) swim bladder area of control, and AFB1-exposed 120 hpf larvae (n = 3 replicates, n = 10 larvae per replicate). Data represent the mean and SD. "*" indicates statistical significance at $p < 0.05$ vs. the control (DMSO).

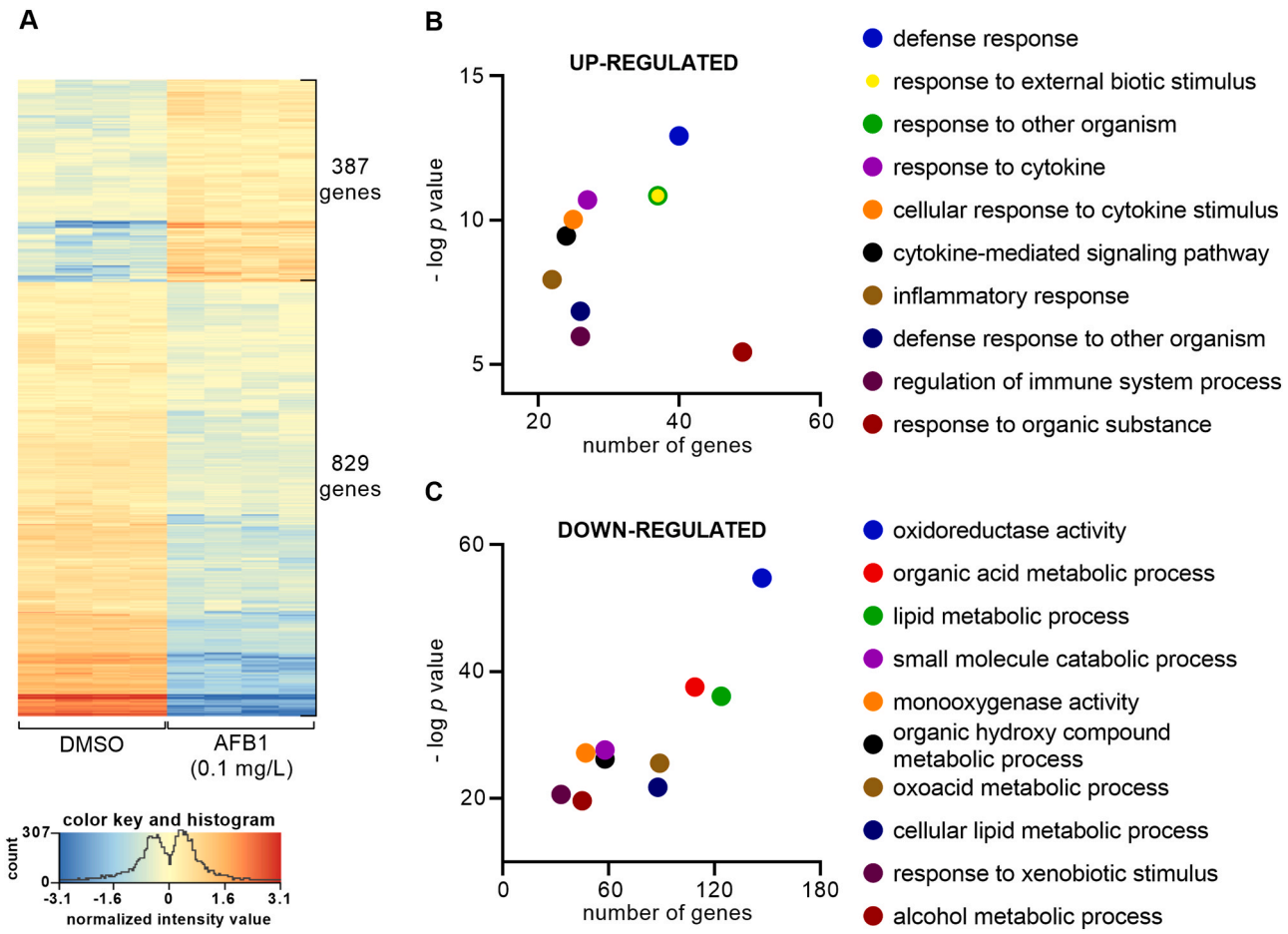

Fig. 2. Embryonic exposure to AFB1 results in global gene expression changes in zebrafish larvae. (A) Heat map showing the differentially expressed genes between the control (DMSO) and the AFB1-exposed (0.1 mg/L) 120 hpf larvae. Data represent the normalized gene expression values of the four independent biological replicates per treatment. (B) Scatter plot showing the top 10 most significantly over-represented Gene Ontology terms among up-regulatedgenes in AFB1-exposed 120 hpf larvae. Y-axis represents the negative log (base 10) of the term significance (*p*-value). X-axis represents the number of genes associated with the term. (C) Scatter plot showing the top 10 most significantly over-represented Gene Ontology terms among down-regulated genes in AFB1-exposed 120 hpf larvae. Y-axis represents the negative log (base 10) of the term significance (*p*-value). X-axis represents the number of genes associated with the term.

2.13. Fluorescence microsphere swallowing assay

Before use, 2.5% fluorescent microbead suspension was washed and reconstituted with reverse osmosis water. 120 hpf larvae from two independent experiments (n = 10 larvae per experiment) were transferred into microcentrifuge tubes (5 larvae/tube) containing 1 mL microbead−water suspension at a final concentration of 0.025%. After 3 h incubation at 25.5 °C, the larvae were washed thoroughly with system water, anesthetized with tricaine methane sulfonate (MS222, 168 mg/l) and imaged under a Leica M205 FA fluorescence microscope using mCherry filter. The quantification of the accumulated microspheres is based on the measurement of the fluorescence intensity in the intestinal tract, including intestinal bulb, middle and posterior intestines (Hama et al., 2009). Intensities of fluorescent signals from the gut were measured in greyscale using ImageJ software.

2.14. Statistical analyses

Data were tested for normality using Shapiro-Wilk test and analyzed with one-way parametric ANOVA followed by post-hoc Dunnett test or Kruskall-Wallis test (non-parametric ANOVA) followed by post-hoc Dunn test using GraphPad Prism 8. Results are presented as the mean ±standard deviation (SD). Differences at the value of $p < 0.05$ were considered statistically significant.

3. Results

3.1. Sub-lethal AFB1 exposure-induced morphological and transcriptional changes in zebrafish larvae

To study the AFB1 exposure-induced adverse effects during the embryonal development of zebrafish, we performed an embryo toxicity test and determined the toxicity values, including LC_1, LC_{10}, and LC_{50} values at 120 hpf (Fig. 1A). LC_1 and LC_{10} value proved to be 0.081 mg/L and 0.108 mg/L, thus we selected a sub-lethal, low concentration range (0.025, 0.05, 0.075, 0.1 mg/L) for the investigation of sub-lethal AFB1 exposure-induced embryonal deformities (Fig. 1A, B). Although dramatic morphological malformations were not observed, AFB1 induced a significant reduction in the total body length at 0.1 mg/L and the swim bladder area in a concentration-dependent manner (Fig. 1C–E).

To further examine the harmful effects of sub-lethal AFB1 exposition, we performed high-throughput RNA-seq analysis identifying the AFB1 exposition-induced gene expression changes in 120 hpf zebrafish larvae. Our global transcriptome analysis identified 1216 significantly differentially expressed genes (DEGs) in response to 0.1 mg/L AFB1 treatment. Among DEGs, 829 genes were down-regulated, and 387 genes showed up-regulation following AFB1 exposition (Fig. 2A; Supplementary Table S2.). To identify the embryonic AFB1 exposition-modulated biological processes, we applied *in silico* GO biological process analysis using Cytoscape's ClueGo application (Bindea et al., 2009). Among the

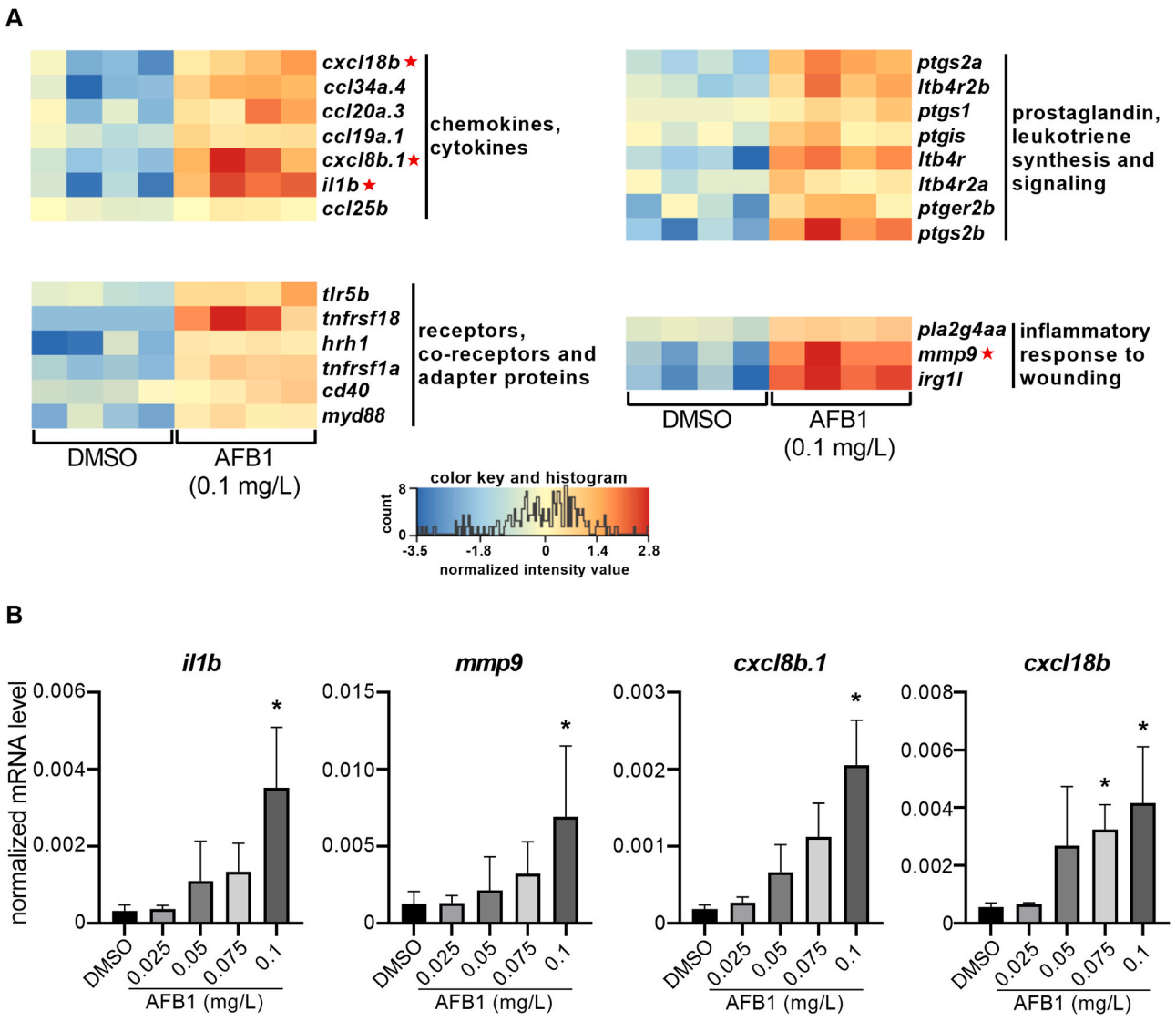

Fig. 3. AFB1 induces the expression of immune- and inflammation-related genes in zebrafish larvae. (A) Heat maps illustrating the significantly up-regulated immune response- and inflammation-associated genes in the AFB1 (0.1 mg/L) -exposed 120 hpf zebrafish larvae compare to the control. Data represent the normalized gene expression values of the four independent biological replicates per treatment. Red asterisks indicate the selected genes for RT-qPCR. (B) RT-qPCR-based gene expression on a set of AFB1-induced inflammatory genes in the AFB1 (0.025–0.1 mg/L) -exposed 120 hpf zebrafish larvae (n = 5 replicates, n = 30 pooled larvae per replicate). Data represent the mean and SD. "*" indicates statistical significance at $p < 0.05$ vs. the control (DMSO).

AFB1-induced genes, various immune response- and inflammation-related functional categories were prominently enriched (Fig. 2B, Supplementary Table S3). In contrast, oxidoreductive processes, organic acid and organic hydroxyl compound metabolism, and lipid metabolism were the most significantly overrepresented biological processes among the AFB1-repressed genes (Fig. 2C, Supplementary Table S3).

Taken together, these findings suggest that sub-lethal AFB1 exposure does not cause dramatic embryonal deformities except for swim bladder area but influences lipid metabolism and the function of the immune system.

3.2. *AFB1-induced inflammatory gene signature associates with abnormal neutrophil granulocyte distribution, number, and migratory capacity*

To further characterize the potential immunomodulatory and pro-inflammatory effects of AFB1, we selected four genes, including interleukin 1 beta (*il1β*), matrix metallopeptidase 9 (*mmp9*), chemokine (C-X-C motif) ligand 8b, duplicate 1 (*cxcl8b.1*), and chemokine (C-X-C motif) ligand 18b (*cxcl18b*) from the immune response-related gene sets (Fig. 3A) and examined their AFB1-regulated expression at the mRNA level in 120 hpf zebrafish larvae using the RT-qPCR method. As expected, AFB1 exposition increased the mRNA expression of each selected gene in a concentration-dependent manner. In the case of three selected genes, including *il1β*, *mmp9*, and *cxcl8b.1*, significant differences could be detected between the control and AFB1-exposed groups at 0.1 mg/L, while in the case of *cxcl18b*, at 0.075 and 0.1 mg/L (Fig. 3B).

The AFB1-induced inflammation-related gene set includes some neutrophil granulocyte chemoattractant factors such as *cxcl8b.1* and *cxcl18b*, raising the possibility of altered neutrophil granulocyte distribution, migration and number in AFB1-exposed zebrafish larvae (de Oliveira et al., 2015; Torraca et al., 2017). To determine whether AFB1 regulates neutrophil granulocyte distribution, we used a neutrophil granulocyte-specific transgenic Tg(mpx:EGFP) zebrafish line. The fluorescent microscopy-based in vivo detection of neutrophil granulocytes demonstrated that sub-lethal AFB1-exposure resulted in a diffuse and widespread neutrophil granulocyte distribution in a

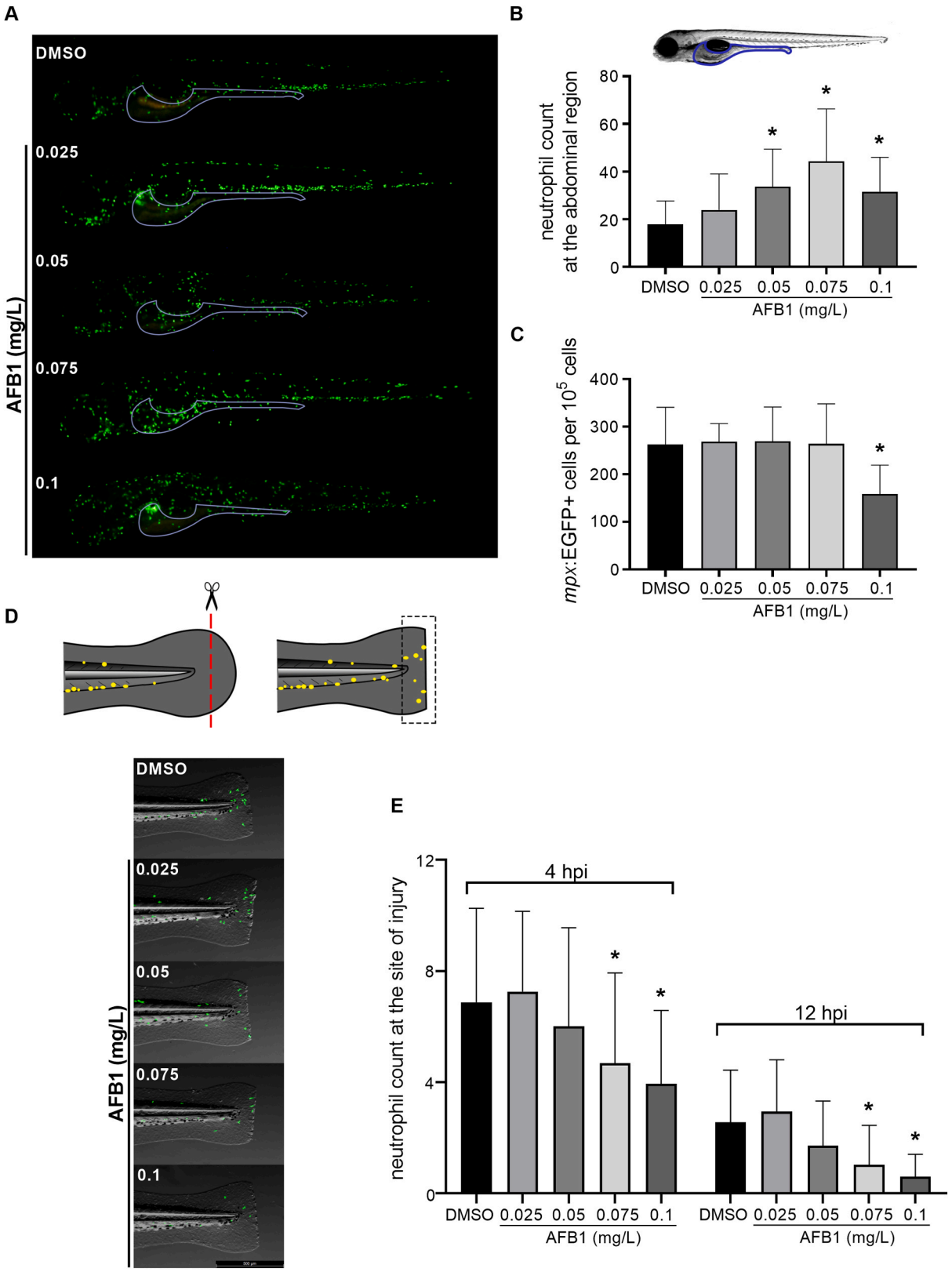

Fig. 4. AFB1 alters the distribution of neutrophil granulocytes and modulates the inflammatory response to a local injury in zebrafish larvae. (A) Representative images of 120 hpf neutrophil-reporter Tg(mpx:EGFP) larvae after embryonic, sub-lethal exposure to AFB1. Scale bar = 500 μm. (B) The number of neutrophils counted in the abdominal region of the control and AFB1-exposed larvae (n = 3 replicates, n = 10 larvae per replicates). (C) Flow cytometric detection of mpx: EGFP+cells per 100.000 cells in control and AFB1-exposed larvae (n = 6 replicates, n = 15 pooled larvae per replicate). (D) Schematic figure of the tail fin transection model and the representative images of the transected fins of control and AFB1-exposed Tg(mpx:EGFP) larvae at 4 h post injury. After tail fin transection, neutrophils started to migrate to the site of injury. Scale bar = 500 μm (E) The graph showing the number of neutrophils at the wound site at 4 h and 12 h post injury (n = 5 replicates, n = 10 larvae per replicate). Data represent the mean and SD. "*" indicates statistical significance at $p < 0.05$ vs. the control (DMSO).

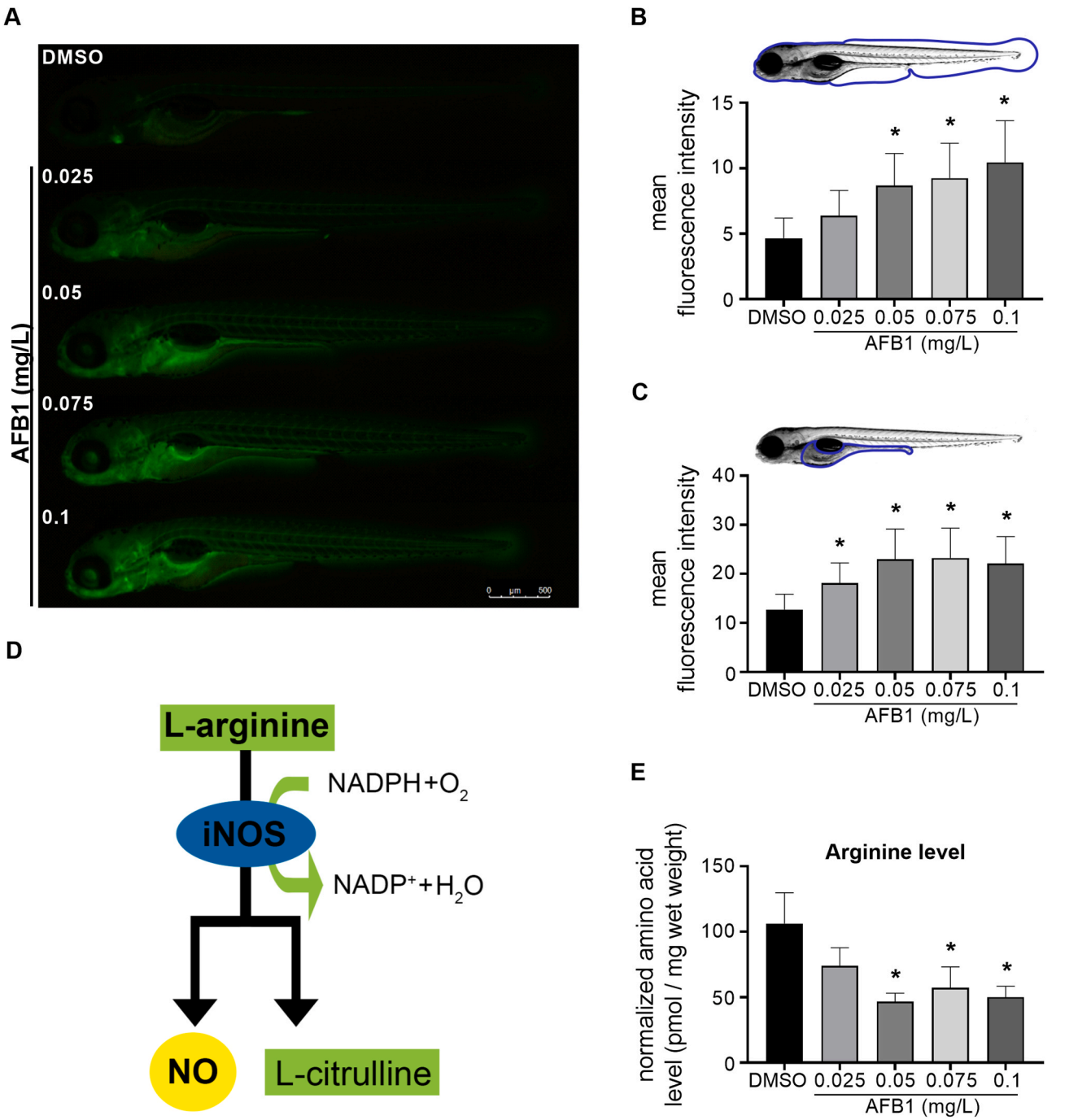

Fig. 5. AFB1 induces nitric oxide production and arginine depletion in zebrafish larvae. (A) Representative fluorescence images of DAF-FM-DA stained 120 hpf larvae after embryonic exposure to AFB1. Fluorescence signals indicate nitric-oxide generation. Scale bar = 500 µm. The graphs showing the mean fluorescence intensities of (B) the whole larvae and (C) the abdominal region (yolk and intestinal area) of the larvae after AFB1 exposure (n = 2 replicates, n = 10 larvae per replicate). (D) Schematic representation of iNOS enzyme-catalyzed NO synthesis. (E)The graph showing the normalized free L-arginine levels of 120 hpf larvae after AFB1 exposure (n = 3 replicates, n = 30 pooled larvae per replicate). Data represent the mean and SD. "*" indicates statistical significance at $p < 0.05$ vs. the control (DMSO).

concentration-dependent manner (Fig. 4A). Additionally, neutrophil granulocytes were observed in huge numbers in the abdominal region of AFB1-exposed zebrafish larvae (Fig. 4A, B). Next, we studied the total neutrophil granulocyte number in AFB1-exposed zebrafish larvae at 120 hpf using flow cytometry analysis (FACS). The FACS analysis revealed that a significant reduction in the GFP positive neutrophil granulocyte number occurred only at the highest (0.1 mg/L) AFB1 concentration (Fig. 4C).

Next, we aimed to examine the potential effects of AFB1 on neutrophil granulocyte migration using the tail fin transection model. After tail fin removal, we determined the number of migrating neutrophil granulocytes to the wound. Our results showed that the number of the migrated neutrophils was decreased significantly in the AFB1-treated 108 hpf larvae at 4 and 12 h after tail fin transection in a concentration-dependent manner (Fig. 4D, E).

These findings indicate that low concentration (≤LC10) AFB1 exposition-induced inflammation is associated with abnormal neutrophil granulocyte distribution, number, and migratory capacity.

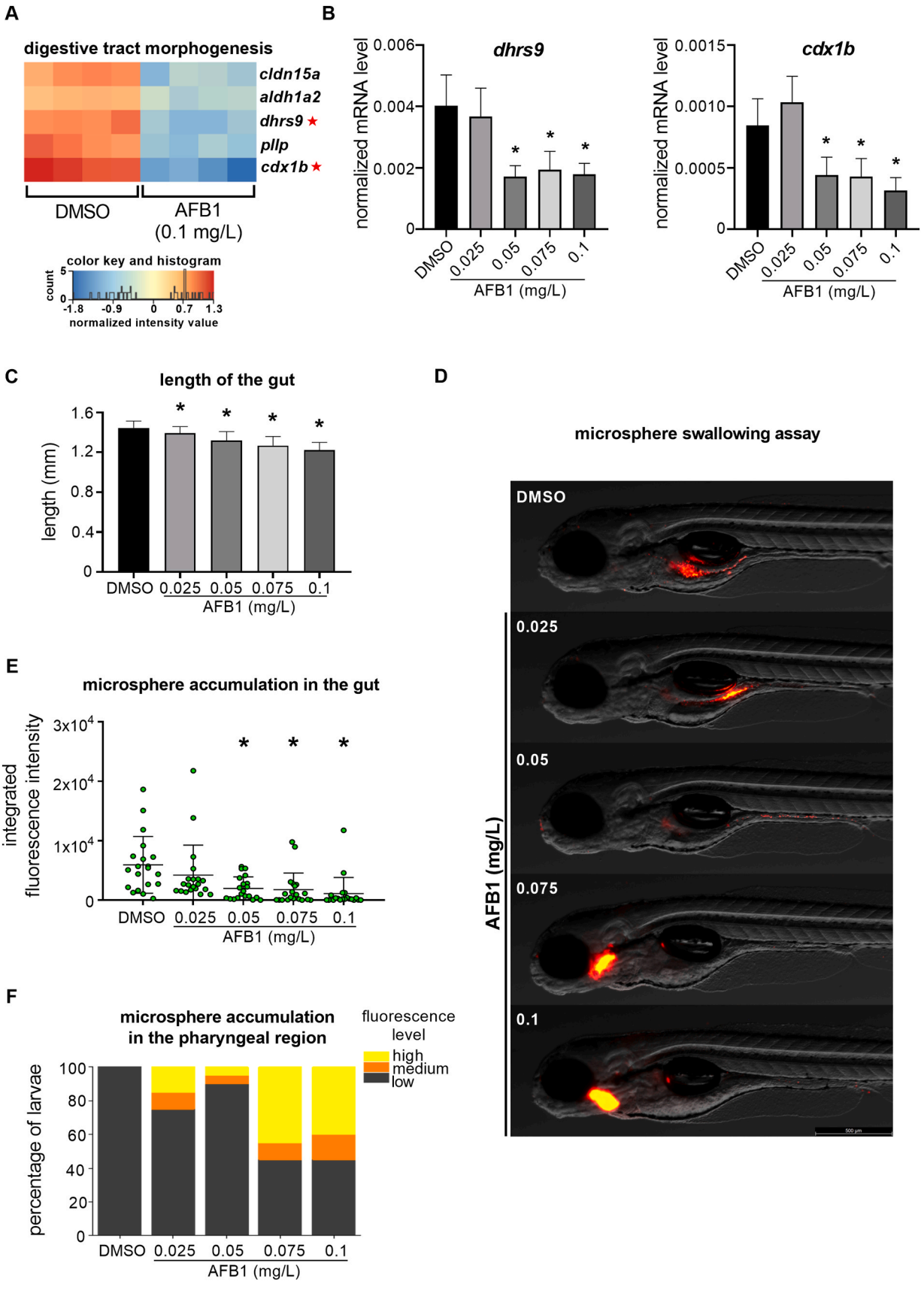

(caption on next page)

Fig. 6. Embryonic exposure to AFB1 impairs gastrointestinal tract development in zebrafish larvae. (A) Heat map illustrating significant down-regulation of digestive tract development-associated gene set in the AFB1 (0.1 mg/L) -exposed 120 hpf zebrafish larvae compared to the control. Data represent the normalized gene expression values of the four independent biological replicates per treatment. Red asterisks indicate the selected genes for RT-qPCR. (B) RT-qPCR-based analysis of 2 selected gastrointestinal tract development-related genes after embryonic exposure to different sub-lethal concentrations of AFB1 (n = 5 replicates, n = 30 pooled larvae per replicate). (C) Length of the larval gut after AFB1 exposure (n = 3 replicates, n = 10 larvae per replicate). (D) Microsphere swallowing assay. Representative images of 120 hpf zebrafish larvae incubated in fluorescence microsphere suspension after AFB1 exposure. Scale bar = 500 μm (E) Scatter plot representing the integrated fluorescence intensities of the swallowed microspheres accumulated in the larval gut after AFB1 exposure (n = 2 replicates, n = 10 larvae per replicate). (F) Proportion of the larvae observed in different fluorescence categories indicating the microsphere accumulation level in the pharyngeal region (n = 2 replicates, n = 10 larvae per replicate). Fluorescence level was categorized as "low" $< 5 \times 10^4$, $5 \times 10^4 <$ "medium" $< 5 \times 10^5$ and $5 \times 10^5 <$ "high" (expressed as the sum of the pixel values). Data represent the mean and SD. "*" indicates statistical significance at $p < 0.05$ vs. the control (DMSO).

3.3. AFB1-induced nitric oxide production is associated with attenuated arginine level

Nitric oxide (NO) is produced by inducible nitric oxide synthase (iNOS) following pathogen infections or xenobiotic-exposures in various innate immune cells (Braun et al., 1999; Jin et al., 2011; Neves-Souza et al., 2005). As an easily detectable molecule, nitric oxide (NO) is a widely used inflammatory marker in different experimental systems, including zebrafish embryos (Cha et al., 2018; Ryu et al., 2015). Therefore, we decided to further characterize the AFB1-induced inflammation with the DAF-FM-DA fluorescent staining-based detection of NO production. As expected, the NO level was significantly increased in the whole body of 120 hpf zebrafish larvae in a concentration-dependent manner by AFB1 (Fig. 5A, B). Like the neutrophil granulocyte distribution, AFB1-induced NO production was the most pronounced in the abdominal region (Fig. 5C). iNOS utilizes L-arginine substrate for NO production (Fig. 5D) (Aktan, 2006). Therefore, we investigated the effect of AFB1 on L-arginine content in whole zebrafish larvae lysates using the AccQ-Tag derivatization method. AFB1 exposure significantly decreased the L-arginine level at 0.05, 0.075, and 0.1 mg/L concentrations (Fig. 5E).

These findings indicate that low concentration (≤LC10) AFB1 exposure-induced inflammation is associated with elevated NO production and reduced L-arginine level.

3.4. AFB1-induced abnormalities in a gastrointestinal tract development

Based on the neutrophil granulocyte distribution pattern and NO production, we hypothesized that the abdominal region is one of the dominant targets of the harmful effects of AFB1 in zebrafish larvae. Besides, our transcriptome analysis identified several AFB1-repressed genes, including claudin 15a (*cldn15a*), aldehyde dehydrogenase 1 family, member A2 (*aldh1a2*), dehydrogenase/reductase (SDR family) member 9 (*dhrs9*), plasmolipin (*pllp*), and caudal type homeobox 1 b (*cdx1b*), which have an essential role in the digestive tract morphogenesis (Fig. 6A). Our RT-qPCR-based validation of *dhrs2* and *cdx1b* expression confirmed that both selected genes were inhibited in a concentration-dependent manner by AFB1 (Fig. 6B). Therefore, we decided to investigate whether AFB1 exposition can influence the size of the larval gut. Thus, we measured the approximate gut length based on the method of Chuang et al. (2019). As expected, embryonic AFB1-exposure significantly decreased the gut length in a concentration-dependent manner (Fig. 6C).

Next, we investigated whether AFB1 can modify the intestinal function in zebrafish larvae. To examine the intestinal function of non-feeding zebrafish larvae, we applied the fluorescence microsphere swallowing assay (Hama et al., 2009). Interestingly, we could detect considerable differences in the fluorescence intensity values in the intestinal tract between the control and the AFB1-treated 120 hpf larvae. On the one hand, significantly reduced microsphere accumulation was observed in the intestinal tract of the AFB1-treated larvae at 0.05, 0.075, and 0.1 mg/L (Fig. 6D and E). On the other hand, 55% of individuals showed a strong microsphere accumulation in the pharyngeal region at 0.075 and 0.1 mg/L (Fig. 6D and F).

Overall, these findings suggest that AFB1-induced abdominal inflammation is associated with abnormal development of the gastrointestinal system.

3.5. AFB1-induced abnormal yolk lipid utilization

Maternally deposited lipids within the yolk play an essential role during embryogenesis, providing an energy source for the developing zebrafish embryo. However, the yolk is not passive lipid storage; it is metabolically active, processing yolk lipids before mobilization to the embryonic body (Fraher et al., 2016). Our transcriptome analysis revealed metabolic pathways, including lipid metabolism and transport as major target processes were repressed by 0.1 mg/L AFB1 exposition (Fig. 2C). In parallel, we found defective gastrointestinal tract development and abdominal inflammation in AFB-exposed 120 hpf zebrafish larvae (Figs. 4A, B; 5A, C, 6) indicating that the abdominal region is strongly affected by AFB1-induced toxicity. Thus, we hypothesized that sub-lethal AFB1 exposition reduces the expression of yolk lipid metabolism and transport-linked genes attenuating the mobilization of yolk lipids during zebrafish embryogenesis.

To test this hypothesis, we first performed a gene set enrichment analysis (GSEA) comparing the AFB1-regulated genes to a lipid metabolism- and transport-associated gene set identified in the zebrafish yolk by Fraher et al. (2016). Our GSEA analysis demonstrated that the yolk-specific lipid metabolism and transport-associated gene set was significantly enriched (FDR q-value < 0.1; NES: - 1.53) among the AFB1-repressed genes (Fig. 7A, B). To investigate the concentration dependency of AFB1-inhibited lipid transport and metabolism-linked gene signature, we selected four AFB1-repressed genes, including microsomal triglyceride transfer protein (*mtp*), apolipoprotein A-IV a (*apoa4a*), apolipoprotein Bb, tandem duplicate 1 (*apobb.1*), and fatty acid binding protein 1b, tandem duplicate 1 (*fabp1b.1*). We measured their mRNA expression in 120 hpf zebrafish larvae after 0.025, 0.05, 0.075, and 0.1 mg/L AFB1 exposure using RT-qPCR method. Each selected gene showed a significantly attenuated expression at 0.05 mg/L AFB1 concentration or higher (Fig. 7C).

To investigate whether the AFB1 exposure-dependent repression of lipid metabolism and transport-associated gene signature results in defective lipid mobilization from the yolk sac, we determined the lipid content and distribution in AFB-exposed 120 hpf zebrafish larvae using ORO staining. As expected, extensive lipid accumulation was observed in the yolk sac of the control and AFB1-exposed zebrafish larvae at 120 hpf, but the lipid content in the abdominal region was significantly increased even at the lowest applied AFB1 concentration suggesting the AFB1-inhibited lipid mobilization from the yolk sac (Fig. 7D, E).

Taken together, these findings indicate that AFB1 can impair lipid utilization during zebrafish embryogenesis even at a sub-lethal concentration resulting in impaired yolk lipid mobilization.

4. Discussion

AFB1 contamination could be detected worldwide in various food and feed ingredients in the last decades, causing severe health problems from domesticated animals to humans. Though AFB1 is known as a carcinogen agent, it has also neurotoxic, immunotoxic and embryotoxic effects (Mahato et al., 2019; Martinez-Miranda et al., 2019; McGlynn

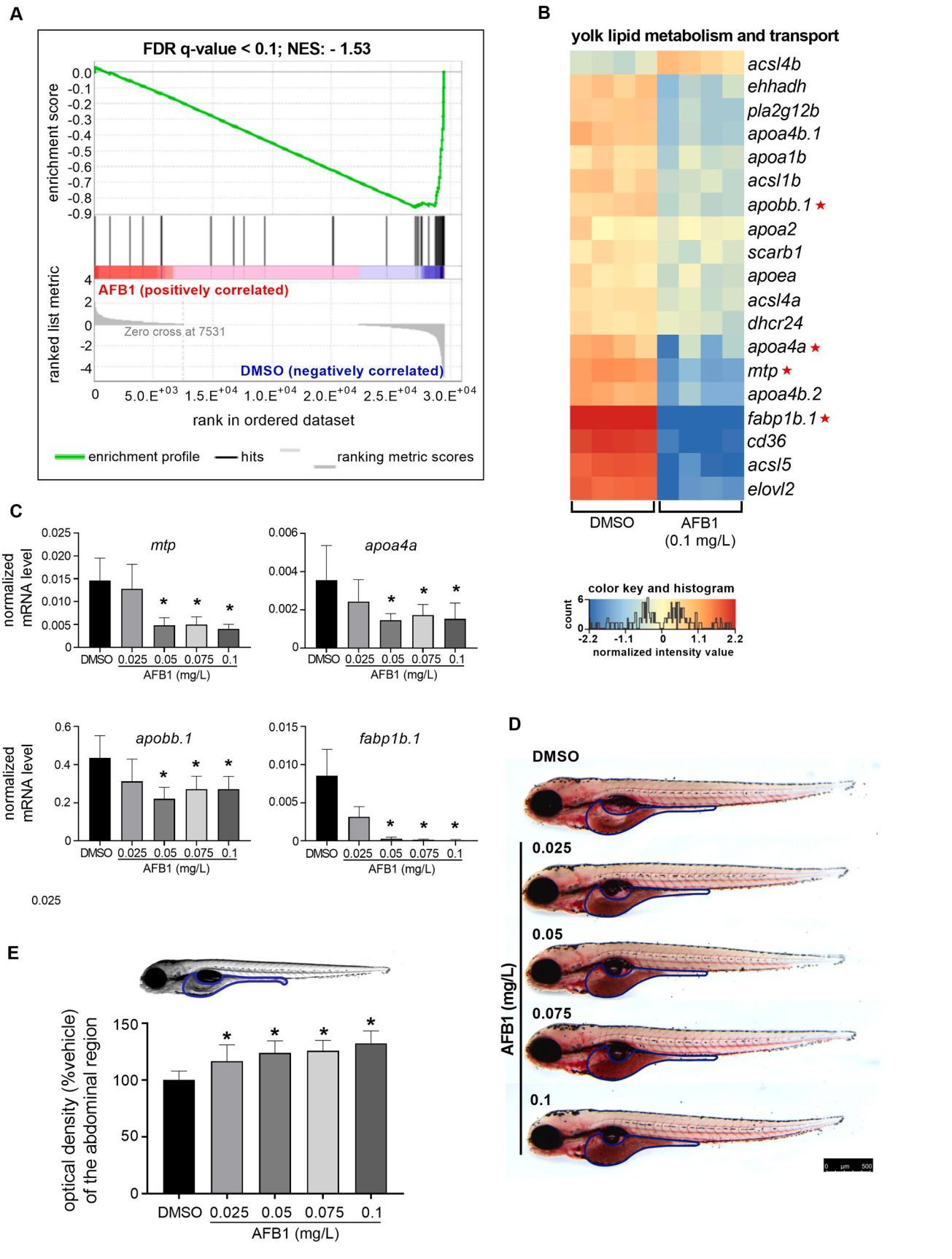

(caption on next page)

Fig. 7. Embryonic exposure to AFB1 disrupts yolk lipid metabolism in zebrafish larvae. (A) Gene set enrichment analysis (GSEA) of lipid metabolism and transport-associated genes in 120 hpf zebrafish larvae exposed to 0.1 mg/L AFB1. The selected lipid-associated genes were identified in the zebrafish yolk by Fraher et al. (2016). FDR: false discovery rate; NES: normalized enrichment score. (B) Heat map illustrating the expression level of 19 lipid-associated genes identified by GSEA between the control and the AFB1-exposed larvae. Data represent the normalized gene expression values of the four independent biological replicates per treatment. Red asterisks indicate the selected genes for RT-qPCR. (C) RT-qPCR-based analysis of four selected yolk lipid metabolism and transport-related genes after embryonic exposure to different sub-lethal concentrations of AFB1 (n = 5 replicates, n = 30 pooled larvae per replicate) (D) Representative images of Oil Red O (ORO) stained 120 hpf larvae after AFB1 exposure. ORO staining indicates the lipid content and distribution in the larvae. Scale bar = 500 μm. (E) Lipid content was evaluated by optical density (OD) measurement. The graph showing OD values of the abdominal region relative to the control (100%) after AFB1 exposure (n = 2 replicates, n = 10 larvae per replicate). Data represent the mean and SD. "*" indicates statistical significance at $p < 0.05$ vs. the control (DMSO).

et al., 2003; Mehrzad et al., 2018; Meissonnier et al., 2008; Park et al., 2020; Wangikar et al., 2005). It has been described that AFB1 exposure during pregnancy induces impaired fetal growth and may increase the risk of pregnancy loss or prematurity (Smith et al., 2017). AFB1 exposure-induced fetal abnormalities may originate from three different mechanisms: (i) indirect maternal toxicities including increased maternal pro-inflammatory cytokine production and impaired nutrient absorption; (ii) placental injuries such as reduced placental mass or elevated placental pro-inflammatory cytokine production and (iii) direct AFB1-caused embryotoxic effects (reviewed in Smith et al., 2017). However, it is difficult to distinguish between the direct and indirect embryotoxic effects of *in utero* exposure to AFB1 in mammals. Despite the obvious differences in fertilization and fetal growth, the high genomic and molecular similarities, as well as the conserved development of several organ systems between mammals and zebrafish, indicating that the lessons learned from various studies in a zebrafish embryo model system may be applicable to humans (Ellett and Lieschke, 2010; Howe et al., 2013; Lieschke and Currie, 2007; Veldman and Lin, 2008; Williams and Hong, 2011; Yuan et al., 2018). Therefore, we investigated the direct AFB1-induced embryotoxicity in a zebrafish embryo model system integrating toxicological, transcriptomic, immunological, and biochemical approaches.

At the applied sub-lethal AFB1 concentrations between 0.025 mg/L and 0.1 mg/L, we did not observe severe morphological deformities in 120 hpf zebrafish larvae consistently with the findings of Wu et al. (2019). Besides, our global transcriptome analysis showed that AFB1-regulates more than a thousand genes at mRNA revel. Among the AFB1-induced genes, the immune and inflammation-related gene sets were the most significantly enriched ones, indicating an immunomodulatory and inflammatory role of AFB1. It has been recently published that AFB1 induces elevated ROS production in the yolk sac area of zebrafish larvae (Dey and Kang, 2020). Similarly to this finding, we could detect increased neutrophil granulocyte number and NO production in the abdominal region of 120 hpf larvae. Interestingly, we found a significant reduction in NO synthesis substrate L-Arginine level in AFB1-exposed larvae indicating that the elevated NO production is associated with the depletion of free L-Arginine storage. Taken together, our results show that AFB1-induces inflammation in zebrafish embryos which is most pronounced in the abdominal region.

Recently, Park et al. (2020) demonstrated that AFB1 exposure between 24 and 48 hpf could significantly enhance yolk sac diameter during zebrafish embryogenesis. These findings raised the possibility that AFB1 exposure can negatively affect the utilization of nutrients from the yolk sac. It has been known that yolk is metabolically active, participating in both the processing and transport of various nutrients including lipids (Fraher et al., 2016). We showed decreased mRNA expression of most yolk sac lipid metabolism-related enzymes and transporters with elevated lipid level in the abdominal region of AFB1-exposed zebrafish larvae indicating the association between lipid accumulation and inflammation. The abnormal lipid accumulation might be associated with inflammation in various diseases, including obesity and non-alcoholic fatty liver disease (de Oliveira et al., 2019; Gao and Tsukamoto, 2016). Furthermore, xenobiotics-induced acute hepatotoxicity may be also related to abnormal lipid accumulation. It has been described that tamoxifen, a selective estrogen receptor modulator, induces increased lipid accumulation and elevated inflammatory gene expression in zebrafish liver (Yu et al., 2020). The acute AFB1-induced hepatotoxicity also involves inflammatory cell infiltration, activation of liver resident Kupffer cells as well as elevated liver cholesterol, triacylglycerol, and phospholipid contents, suggesting a tight connection between pathological lipid accumulation and inflammation (Lu et al., 2013; Rotimi et al., 2017; Ugbaja et al., 2020; Zhang et al., 2019). Nevertheless, in the case of AFB1-induced abdominal lipid accumulation and inflammation in zebrafish larvae, it remains to be elucidated whether AFB1-induced inflammation inhibits lipid utilization or AFB1 attenuates lipid absorption leading to enhanced inflammation.

It has been demonstrated that AFB1 reduces intestinal barrier function and causes dysregulation of gut microbiota in vertebrates, but its adverse effects on gastrointestinal tract development are not fully understood (Hernández-Ramírez et al., 2020; Wang et al., 2016; Yang et al., 2017; Yunus et al., 2011). Our transcriptome analysis identified an AFB1-attenuated gene set including *cldn15a*, *aldh12a*, *dhrs9*, *pllp*, and *cdx1b*, which are essential for proper gastrointestinal tract development (Bagnat et al., 2007; Flores et al., 2008; Nadauld et al., 2005; Pittlik and Begemann, 2012; Rodríguez-Fraticelli et al., 2015). We found a significant reduction in gut length and abnormalities in intestinal function in AFB1-exposed zebrafish larvae according to the gene expression changes. These results collectively support the hypothesis that AFB1 can impair gastrointestinal development, but the exact molecular mechanisms remain unclear.

It has been previously described that maternal AFB1 exposure may increase the risk of adverse birth outcomes, including low birth weight (Lauer et al., 2019; Shuaib et al., 2010). AFB1-impaired growth was also observed in 1–5 years old children in West Africa (Gong et al., 2008; Lauer et al., 2019). However, the molecular background of AFB1-impaired growth of the fetus and young children is currently unknown (Gong et al., 2008; Lauer et al., 2019; Shuaib et al., 2010). In our zebrafish embryo model, AFB1-induced inflammation, diminished lipid transport, and abnormal gastrointestinal tract development were also associated with the slight but significant reduction in the body length at the highest (0.1 mg/L) applied AFB1 concentration. Interestingly, the AFB1 exposure-affected biological processes show remarkably conserved regulation in zebrafish and mammals. For instance, the gene regulation program of acute inflammation in zebrafish highly resembles one observed in mammals (Forn-Cuní et al., 2017). Regulatory and metabolic pathways for gastrointestinal tract development as well as nutrient uptake and transport are also highly conserved in zebrafish and mammals (Flynn III et al., 2009; Marza et al., 2005; Miyares et al., 2014; Quinlivan and Farber, 2017; Wallace and Pack, 2003). Nevertheless, the question is currently open whether the disorders of the gastrointestinal tract or lipid transport may underlie the AFB1-induced low birth-weight and growth faltering in young children.

In conclusion, this study supports that exposure to relatively low concentrations of AFB1 has a complex direct embryotoxic effect in the zebrafish embryo model system. Although AFB1 does not induce dramatic developmental abnormalities at the applied concentrations but causes elevated inflammation and abnormal lipid accumulation in the abdominal area. Moreover, gastrointestinal disorders were observed in AFB1-exposed zebrafish larvae, which were characterized by reduced gut length and functional abnormalities. Data presented herein can provide more information for estimating the direct embryotoxicity of

AFB1 and a useful, cost-effective vertebrate model system for developing various AFB1-mediated embryotoxicity-reducing strategies.

CRediT authorship contribution statement

B.I., B.U., and Z.C. directed the study and wrote the manuscript. B.I., G.G., M.R., B.I., M.T., A.D., B.N., A.S., M.C., E.C., A.B., Z.C.B. and A.A performed the experiments. S.P. directed the sequencing and bioinformatic analyses.

Declaration of Competing Interest

The authors declare that they have no known competing financial interests or personal relationships that could have appeared to influence the work reported in this paper.

Acknowledgements

This work was supported by National Development and Innovation Fund (NKFIHH); Grant Agreement: NVKP_16-1-2016-0009, NVKP_16–1-2016-0035, GINOP-2.3.4-15-2016-00002, KP2020-NKA-16, EFOP-3.6.3-VEKOP-16-2017-00008 project cofinanced by the European Union, and the Thematic Excellence Program TKP2020-NKA-16 of Szent Istvan University, awarded by Ministry for Innovation and Technology and supported by the UNKP-20–3-II New National Excellence Program of the Ministry for Innovation and Technology. Zsolt Csenki was supported by the Janos Bolyai Research Grant (BO/00669/20/4) of the Hungarian Academy of Sciences. Zsolt Czimmerer was supported by the Premium Postdoctoral Fellowship Program of the Hungarian Academy of Sciences.

The authors thank Professor Miklós Mézes for proofreading the manuscript. The technical help of Renáta Kovács is greatly acknowledged.

Appendix A. Supporting information

Supplementary data associated with this article can be found in the online version at doi:10.1016/j.jhazmat.2021.125788.

References

Abdulrazzaq, Y.M., Osman, N., Ibrahim, A., 2002. Fetal exposure to aflatoxins in the United Arab Emirates. Ann. Trop. Paediatr. 22, 3–9. https://doi.org/10.1179/027249302125000094.

Aktan, F., 2006. iNOS-mediated nitric oxide production and its regulation. Life Sci. 75, 639–653. https://doi.org/10.1016/j.lfs.2003.10.042.

Anderson, J.L., Carten, J.D., Farber, S.A., 2011. Zebrafish Lipid Metabolism: From Mediating Early Patterning to the Metabolism of Dietary Fat and Cholesterol, Third ed. Elsevier Ltd. https://doi.org/10.1016/B978-0-12-387036-0.00005-0

Bagnat, M., Cheung, I.D., Mostov, K.E., Stainier, D.Y.R., 2007. Genetic control of single lumen formation in the zebrafish gut. Nat. Cell Biol. 9, 954–960. https://doi.org/10.1038/ncb1621.

Barr, D.B., Bishop, A., Needham, L.L., 2007. Concentrations of xenobiotic chemicals in the maternal-fetal unit. Reprod. Toxicol. 23, 260–266. https://doi.org/10.1016/j.reprotox.2007.03.003.

Battilani, P., Leggieri, C.M., 2015. Predictive modelling of aflatoxin contamination to support maize chain management. World Mycotoxin J. 8, 161–170. https://doi.org/10.3920/WMJ2014.1740.

Battilani, P., Rossi, V., Giorni, P., Pietri, A., Gualla, A., Van der Fels-Klerx, H.J., Booij, C. J.H., Moretti, A., Logrieco, A., Miglietta, F., Toscano, P., Miraglia, M., De Santis, B., Brera, C., 2012. Modelling, predicting and mapping the emergence of aflatoxins in cereals in the EU due to climate change. EFSA Support. Publ. 9, 223E. https://doi.org/10.2903/sp.efsa.2012.EN-223.

Battilani, P., Toscano, P., Van Der Fels-Klerx, H.J., Moretti, A., Camardo Leggieri, M., Brera, C., Rortais, A., Goumperis, T., Robinson, T., 2016. Aflatoxin B 1 contamination in maize in Europe increases due to climate change. Sci. Rep. 6, 1–7. https://doi.org/10.1038/srep24328.

Bindea, G., Mlecnik, B., Hackl, H., Charoentong, P., Tosolini, M., Kirilovsky, A., Fridman, W.H., Pagès, F., Trajanoski, Z., Galon, J., 2009. ClueGO: a Cytoscape plug-in to decipher functionally grouped gene ontology and pathway annotation networks. Bioinformatics 25, 1091–1093. https://doi.org/10.1093/bioinformatics/btp101.

Braun, J.S., Novak, R., Gao, G., Murray, P.J., Shenep, J.L., 1999. Pneumolysin, a protein toxin of streptococcus pneumoniae, induces nitric oxide production from macrophages. Infect. Immun. 67, 3750–3756.

Cha, S.H., Hwang, Y., Kim, K.N., Jun, H.S., 2018. Palmitate induces nitric oxide production and inflammatory cytokine expression in zebrafish. Fish. Shellfish Immunol. 79, 163–167. https://doi.org/10.1016/j.fsi.2018.05.025.

Cheng, B., Zhang, H., Hu, J., Peng, Y., Yang, J., Liao, X., Liu, F., Guo, J., Hu, C., Lu, H., 2020. The immunotoxicity and neurobehavioral toxicity of zebrafish induced by famoxadone-cymoxanil. Chemosphere 247, 125870. https://doi.org/10.1016/j.chemosphere.2020.125870.

Chuang, L. shiang, Morrison, J., Hsu, N. yun, Labrias, P.R., Nayar, S., Chen, E., Villaverde, N., Facey, J.A., Boschetti, G., Giri, M., Castillo-Martin, M., Thin, T.H., Sharma, Y., Chu, J., Cho, J.H., 2019. Zebrafish modeling of intestinal injury, bacterial exposures and medications defines epithelial in vivo responses relevant to human inflammatory bowel disease. Dis. Model. Mech. 12, dmm037432 https://doi.org/10.1242/dmm.037432.

Dey, D.K., Kang, S.C., 2020. Aflatoxin B1 induces reactive oxygen species-dependent caspase-mediated apoptosis in normal human cells, inhibits Allium cepa root cell division, and triggers inflammatory response in zebrafish larvae. Sci. Total Environ. 737, 139704 https://doi.org/10.1016/j.scitotenv.2020.139704.

Dufour-Rainfray, D., Vourc'h, P., Tourlet, S., Guilloteau, D., Chalon, S., Andres, C.R., 2011. Fetal exposure to teratogens: evidence of genes involved in autism. Neurosci. Biobehav. Rev. 35, 1254–1265. https://doi.org/10.1016/j.neubiorev.2010.12.013.

El-Azab, S.M., Abdelhamid, A.M., Shalaby, H.A., Mehrim, A.I., Ibrahim, A.H., 2010. Study of aflatoxin B1 as a risk factor that impairs the reproductive performance in females - Egypt. Toxicol. Environ. Chem. 92, 383–389. https://doi.org/10.1080/02772240902927510.

Ellett, F., Lieschke, G.J., 2010. Zebrafish as a model for vertebrate hematopoiesis. Curr. Opin. Pharmacol. 10, 563–570. https://doi.org/10.1016/j.coph.2010.05.004.

El-Nahla, S.M., Imam, H.M., Moussa, E.A., Ibrahim, A.M., Ghanam, A.R., 2013. Teratogenic effects of aflatoxin in Rabbits (Oryctolagus cuniculus). J. Vet. Anat. 6, 67–85. https://doi.org/10.21608/jva.2013.45024.

Fang, L., Liu, C., Miller, Y.I., 2014. Zebrafish models of dyslipidemia: Relevance to atherosclerosis and angiogenesis. Transl. Res. 163, 99–108. https://doi.org/10.1016/j.trsl.2013.09.004.

Flores, M.V.C., Hall, C.J., Davidson, A.J., Singh, P.P., Mahagaonkar, A.A., Zon, L.I., Crosier, K.E., Crosier, P.S., 2008. Intestinal differentiation in zebrafish requires Cdx1b, a functional equivalent of mammalian Cdx2. Gastroenterology 135, 1665–1675. https://doi.org/10.1053/j.gastro.2008.07.024.

Flynn III, E.J., Trent, C.M., Rawls, J.F., 2009. Ontogeny and nutritional control of adipogenesis in zebrafi sh (Danio rerio). J. Lipid Res. 50, 1641–1652. https://doi.org/10.1194/jlr.M800590-JLR200.

Forn-Cuní, G., Varela, M., Pereiro, P., Novoa, B., Figueras, A., 2017. Conserved gene regulation during acute inflammation between zebrafish and mammals. Sci. Rep. 7, 1–9. https://doi.org/10.1038/srep41905.

Fraher, D., Sanigorski, A., Mellett, N.A., Meikle, P.J., Sinclair, A.J., Gibert, Y., 2016. Zebrafish embryonic lipidomic analysis reveals that the yolk cell is metabolically active in processing lipid. Cell Rep. 14, 1317–1329. https://doi.org/10.1016/j.celrep.2016.01.016.

Gao, B., Tsukamoto, H., 2016. Inflammation in alcoholic and nonalcoholic fatty liver disease: friend or foe? Gastroenterology 150, 1704–1709. https://doi.org/10.1053/j.gastro.2016.01.025.

Gomes, M.C., Mostowy, S., 2020. The case for modeling human infection in zebrafish. Trends Microbiol 28, 10–18. https://doi.org/10.1016/j.tim.2019.08.005.

Gong, Y.Y., Turner, P.C., Hall, A.J., Wild, C.P., 2008. Aflatoxin exposure and impaired child growth in West Africa: an unexplored international public health burden. In: Leslie, J.F., Bandyopadhyay, R., Visconti, A. (Eds.), Mycotoxins: Detection Methods, Management, Public Health and Agricultural Trade. Cromwell Press, pp. 53–65. https://doi.org/10.1079/9781845930820.0359.

Gong, Y.Y., Watson, S., Routledge, M.N., 2016. Aflatoxin exposure and associated human health effects, a review of epidemiological studies. Food Saf. 4, 14–27. https://doi.org/10.14252/foodsafetyfscj.2015026.

Hama, K., Provost, E., Baranowski, T.C., Rubinstein, A.L., Anderson, J.L., Leach, S.D., Farber, S.A., 2009. In vivo imaging of zebrafish digestive organ function using multiple quenched fluorescent reporters. Am. J. Physiol. Gastrointest. Liver Physiol. 296, 445–453. https://doi.org/10.1152/ajpgi.90513.2008.

Hernández-Ramírez, J.O., Nava-Ramírez, M.J., Merino-Guzmán, R., Téllez-Isaías, G., Vázquez-Durán, A., Méndez-Albores, A., 2020. The effect of moderate-dose aflatoxin B1 and Salmonella Enteritidis infection on intestinal permeability in broiler chickens. Mycotoxin Res. 36, 31–39. https://doi.org/10.1007/s12550-019-00367-7.

Howe, K., Clark, M.D., Torroja, C.F., Torrance, J., Berthelot, C., Muffato, M., Collins, J.E., Humphray, S., McLaren, K., Matthews, L., McLaren, S., Stemple, D.L., 2013. The zebrafish reference genome sequence and its relationship to the human genome. Nature 496, 498–503. https://doi.org/10.1038/nature12111.

Huang, B., Jiang, C., Luo, J., Cui, Y., Qin, L., Liu, J., 2014. Maternal exposure to bisphenol A may increase the risks of Parkinson's disease through down-regulation of fetal IGF-1 expression. Med. Hypotheses 82, 245–249. https://doi.org/10.1016/j.mehy.2013.10.023.

Hussein, H.S., Brasel, J.M., 2001. Toxicity, metabolism, and impact of mycotoxins on humans and animals. Toxicology 167, 101–134. https://doi.org/10.1016/S0300-483X(01)00471-1.

IARC, 1993. Some naturally occurring substances: food items and constituents, heterocyclic aromatic amines and mycotoxins. In: IARC Working Group on the Evaluation of Carcinogenic Risks to Humans. International Agency for Research on Cancer & World Health Organization.

Iwanami, N., 2014. Zebrafish as a model for understanding the evolution of the vertebrate immune system and human primary immunodeficiency. Exp. Hematol. 42, 697–706. https://doi.org/10.1016/j.exphem.2014.05.001.
Jiang, Y., Jolly, P.E., Ellis, W.O., Wang, J.S., Phillips, T.D., Williams, J.H., 2005. Aflatoxin B1 albumin adduct levels and cellular immune status in Ghanaians. Int. Immunol. 17, 807–814. https://doi.org/10.1093/intimm/dxh262.
Jin, Y., Zheng, S., Fu, Z., 2011. Embryonic exposure to cypermethrin induces apoptosis and immunotoxicity in zebrafish (Danio rerio). Fish Shellfish Immunol. 30, 1049–1054. https://doi.org/10.1016/j.fsi.2011.02.001.
Lauer, J.M., Duggan, C.P., Ausman, L.M., Griffiths, J.K., Webb, P., Wang, J.S., Xue, K.S., Agaba, E., Nshakira, N., Ghosh, S., 2019. Maternal aflatoxin exposure during pregnancy and adverse birth outcomes in Uganda. Matern. Child Nutr. 15, e12701 https://doi.org/10.1111/mcn.12701.
Lieschke, G.J., Currie, P.D., 2007. Animal models of human disease: zebrafish swim into view. Nat. Rev. Genet. 8, 353–367. https://doi.org/10.1038/nrg2091.
Lu, X., Hu, B., Shao, L., Tian, Y., Jin, T., Jin, Y., Ji, S., Fan, X., 2013. Integrated analysis of transcriptomics and metabonomics profiles in aflatoxin B1-induced hepatotoxicity in rat. Food Chem. Toxicol. 55, 444–455. https://doi.org/10.1016/j.fct.2013.01.020.
Mahato, D.K., Lee, K.E., Kamle, M., Devi, S., Dewangan, K.N., Kumar, P., Kang, S.G., 2019. Aflatoxins in food and feed: an overview on prevalence, detection and control strategies. Front. Microbiol. 10, 2266. https://doi.org/10.3389/fmicb.2019.02266.
Marroquín-Cardona, A.G., Johnson, N.M., Phillips, T.D., Hayes, A.W., 2014. Mycotoxins in a changing global environment - a review. Food Chem. Toxicol. 69, 220–230. https://doi.org/10.1016/j.fct.2014.04.025.
Martinez-Miranda, M.M., Rosero-Moreano, M., Taborda-Ocampo, G., 2019. Occurrence, dietary exposure and risk assessment of aflatoxins in arepa, bread and rice. Food Control 98, 359–366. https://doi.org/10.1016/j.foodcont.2018.11.046.
Marza, E., Barthe, C., Andre, M., Villeneuve, L., Helou, C., Babin, P.J., 2005. Developmental expression and nutritional regulation of a zebrafish gene homologous to mammalian microsomal triglyceride transfer protein large subunit. Dev. Dyn. Off. Publ. Am. Assoc. Anat. 232, 506–518. https://doi.org/10.1002/dvdy.20251.
Mathias, J.R., Perrin, B.J., Liu, T.-X., Kanki, J., Look, A.T., Huttenlocher, A., 2006. Resolution of inflammation by retrograde chemotaxis of neutrophils in transgenic zebrafish. J. Leukoc. Biol. 80, 1281–1288. https://doi.org/10.1189/jlb.0506346.
Matthews, M., Varga, Z.M., 2012. Anesthesia and euthanasia in zebrafish. ILAR J. 53, 192–204. https://doi.org/10.1093/ilar.53.2.192.
McGlynn, K.A., Hunter, K., LeVoyer, T., Roush, J., Wise, P., Michielli, R.A., Shen, F.M., Evans, A.A., London, W.T., Buetow, K.H., 2003. Susceptibility to aflatoxin B1-related primary hepatocellular carcinoma in mice and humans. Cancer Res. 63, 4594–4601.
Medina, A., Rodriguez, A., Magan, N., 2014. Effect of climate change on Aspergillus flavus and aflatoxin B1 production. Front. Microbiol. 5, 348. https://doi.org/10.3389/fmicb.2014.00348.
Meeker, N.D., Trede, N.S., 2008. Immunology and zebrafish: Spawning new models of human disease. Dev. Comp. Immunol. 32, 745–757. https://doi.org/10.1016/j.dci.2007.11.011.
Mehrzad, J., Bahari, A., Bassami, M.R., Mahmoudi, M., Dehghani, H., 2018. Data on environmentally relevant level of aflatoxin B1-induced human dendritic cells' functional alteration. Data Br. 18, 1576–1580. https://doi.org/10.1016/j.dib.2018.04.104.
Meissonnier, G.M., Pinton, P., Laffitte, J., Cossalter, A.M., Gong, Y.Y., Wild, C.P., Bertin, G., Galtier, P., Oswald, I.P., 2008. Immunotoxicity of aflatoxin B1: Impairment of the cell-mediated response to vaccine antigen and modulation of cytokine expression. Toxicol. Appl. Pharmacol. 231, 142–149. https://doi.org/10.1016/j.taap.2008.04.004.
Mitchell, N.J., Bowers, E., Hurburgh, C., Wu, F., 2016. Potential economic losses to the US corn industry from aflatoxin contamination. Food Addit. Contam. Part A 33, 540–550. https://doi.org/10.1080/19440049.2016.1138545.
Miyares, R.L., De Rezende, V.B., Farber, S.A., 2014. Zebrafish yolk lipid processing: a tractable tool for the study of vertebrate lipid transport and metabolism. DMM Dis. Model. Mech. 7, 915–927. https://doi.org/10.1242/dmm.015800.
Nadauld, L.D., Shelton, D.N., Chidester, S., Yost, H.J., Jones, D.A., 2005. The zebrafish retinol dehydrogenase, rdh1l, is essential for intestinal development and is regulated by the tumor suppressor adenomatous Polyposis coli. J. Biol. Chem. 280, 30490–30495. https://doi.org/10.1074/jbc.M504973200.
Neves-Souza, P.C.F., Azeredo, E.L., Zagne, S.M.O., Valls-de-souza, R., Reis, S.R.N.I., Cerqueira, D.I.S., Nogueira, R., Kubelka, C.F., 2005. Inducible nitric oxide synthase (iNOS) expression in monocytes during acute Dengue Fever in patients and during in vitro infection. BMC Infect. Dis. 5, 1–12. https://doi.org/10.1186/1471-2334-5-64.
OECD, 2013. Test No. 236: fish embryo acute toxicity (FET) test. In: OECD Guidelines for the Testing of Chemicals, Section 2. OECD Publishing, Paris. https://doi.org/10.1787/9789264203709-en.
Oehlers, S.H., Flores, M.V., Hall, C.J., Okuda, K.S., Sison, J.O., Crosier, K.E., Crosier, P.S., 2013. Chemically induced intestinal damage models in zebrafish larvae. Zebrafish 10, 184–193. https://doi.org/10.1089/zeb.2012.0824.
de Oliveira, J.R., Favarin, D.C., Tanaka, S.C.S.V., Balarin, M.A.S., Silva Teixeira, D.N., Levy, B.D., Rogério, A.D.P., 2015. AT-RvD1 modulates CCL-2 and CXCL-8 production and NF-κB, STAT-6, SOCS1, and SOCS3 expression on bronchial epithelial cells stimulated with IL-4. BioMed. Res. Int. 2015, 1–8. https://doi.org/10.1155/2015/178369.
de Oliveira, S., Houseright, R.A., Graves, A.L., Golenberg, N., Korte, B.G., Miskolci, V., Huttenlocher, A., 2019. Metformin modulates innate immune-mediated inflammation and early progression of NAFLD-associated hepatocellular carcinoma in zebrafish. J. Hepatol. 70, 710–721. https://doi.org/10.1016/j.jhep.2018.11.034.
Park, S., Lee, J.Y., You, S., Song, G., Lim, W., 2020. Neurotoxic effects of aflatoxin B1 on human astrocytes in vitro and on glial cell development in zebrafish in vivo. J. Hazard. Mater. https://doi.org/10.1016/j.jhazmat.2019.121639.
Partanen, H.A., El-Nezami, H.S., Leppänen, J.M., Myllynen, P.K., Woodhouse, H.J., Vähäkangas, K.H., 2010. Aflatoxin B1 transfer and metabolism in human placenta. Toxicol. Sci. 113, 216–225. https://doi.org/10.1093/toxsci/kfp257.
Pittlik, S., Begemann, G., 2012. New sources of retinoic acid synthesis revealed by live imaging of an Aldh1a2-GFP reporter fusion protein throughout zebrafish development. Dev. Dyn. 241, 1205–1216. https://doi.org/10.1002/dvdy.23805.
Quinlivan, V.H., Farber, S.A., 2017. Lipid uptake, metabolism, and transport in the larval zebrafish. Front. Endocrinol. 8, 319. https://doi.org/10.3389/fendo.2017.00319.
Reddy, R.V., Taylor, M.J., Sharma, R.P., 1987. Studies of immune function of CD-1 mice exposed to aflatoxin B1. Toxicology 43, 123–132. https://doi.org/10.1016/0300-483X(87)90002-3.
Renshaw, S.A., Loynes, C.A., Trushell, D.M.I., Elworthy, S., Ingham, P.W., Whyte, M.K.B., 2006. A transgenic zebrafish model of neutrophilic inflammation. Blood 108, 3976–3978. https://doi.org/10.1182/blood-2006-05-024075.
Ribas-Fitó, N., Torrent, M., Carrizo, D., Muñoz-Ortiz, L., Júlvez, J., Grimalt, J.O., Sunyer, J., 2006. In utero exposure to background concentrations of DDT and cognitive functioning among preschoolers. Am. J. Epidemiol. 164, 955–962. https://doi.org/10.1093/aje/kwj299.
Rodríguez-Fraticelli, A.E., Bagwell, J., Bosch-Fortea, M., Boncompain, G., Reglero-Real, N., García-León, M.J., Andrés, G., Toribio, M.L., Alonso, M.A., Millán, J., Perez, F., Bagnat, M., Martín-Belmonte, F., 2015. Developmental regulation of apical endocytosis controls epithelial patterning in vertebrate tubular organs. Nat. Cell Biol. 17, 241–250. https://doi.org/10.1038/ncb3106.
Rotimi, O.A., Rotimi, S.O., Duru, C.U., Ebebeinwe, O.J., Abiodun, A.O., Oyeniyi, B.O., Faduyile, F.A., 2017. Acute aflatoxin B1 – Induced hepatotoxicity alters gene expression and disrupts lipid and lipoprotein metabolism in rats. Toxicol. Rep. 4, 408–414. https://doi.org/10.1016/j.toxrep.2017.07.006.
Ryu, S.J., Choi, H.S., Yoon, K.Y., Lee, O.H., Kim, K.J., Lee, B.Y., 2015. Oleuropein suppresses LPS-induced inflammatory responses in RAW 264.7 cell and zebrafish. J. Agric. Food Chem. 63, 2098–2105. https://doi.org/10.1021/jf505894b.
Schlegel, A., Stainier, D.Y.R., 2006. Microsomal triglyceride transfer protein is required for yolk lipid utilization and absorption of dietary lipids in zebrafish larvae. Biochemistry 45, 15179–15187. https://doi.org/10.1021/bi0619268.
Schneider, C.A., Rasband, W.S., Eliceiri, K.W., 2012. NIH Image to ImageJ: 25 years of image analysis. Nat. Methods 9, 671–675. https://doi.org/10.1038/nmeth.2089.
Scholz, S., Fischer, S., Gündel, U., Küster, E., Luckenbach, T., Voelker, D., 2008. The zebrafish embryo model in environmental risk assessment - applications beyond acute toxicity testing. Environ. Sci. Pollut. Res. 15, 394–404. https://doi.org/10.1007/s11356-008-0018-z.
Schönfelder, G., Flick, B., Mayr, E., Talsness, C., Paul, M., Chahoud, I., 2002. In utero exposure to low doses of bisphenol A lead to long-term deleterious effects in the vagina. Neoplasia 4, 98–102. https://doi.org/10.1038/sj.neo.7900212.
Selgrade, M.K., Blain, R.B., Fedak, K.M., Cawley, M.A., 2013. Potential risk of asthma associated with in utero exposure to xenobiotics. Birth Defects Res. Part C. Embryo Today Rev. 99, 1–13. https://doi.org/10.1002/bdrc.21028.
Seth, A., Stemple, D.L., Barroso, I., 2013. The emerging use of zebrafish to model metabolic disease. DMM Dis. Model. Mech. 6, 1080–1088. https://doi.org/10.1242/dmm.011346.
Shirai, S., Suzuki, Y., Yoshinaga, J., Mizumoto, Y., 2010. Maternal exposure to low-level heavy metals during pregnancy and birth size. J. Environ. Sci. Heal. Part A 45, 1468–1474. https://doi.org/10.1080/10934529.2010.500942.
Shuaib, F.M.B., Jolly, P.E., Ehiri, J.E., Yatich, N., Jiang, Y., Funkhouser, E., Person, S.D., Wilson, C., Ellis, W.O., Wang, J.S., Williams, J.H., 2010. Association between birth outcomes and aflatoxin B1 biomarker blood levels in pregnant women in Kumasi. Ghana. Trop. Med. Int. Heal. 15, 160–167. https://doi.org/10.1111/j.1365-3156.2009.02435.x.
Smith, L.E., Prendergast, A.J., Turner, P.C., Humphrey, J.H., Stoltzfus, R.J., 2017. Aflatoxin exposure during pregnancy, maternal anemia, and adverse birth outcomes. Am. J. Trop. Med. Hyg. 96, 770–776. https://doi.org/10.4269/ajtmh.16-0730.
Sun, L., Ling, Y., Jiang, J., Wang, D., Wang, J., Li, J., Wang, X., Wang, H., 2020. Differential mechanisms regarding triclosan vs. bisphenol A and fluorene-9-bisphenol induced zebrafish lipid-metabolism disorders by RNA-seq. Chemosphere 251, 126318. https://doi.org/10.1016/j.chemosphere.2020.126318.
Supriya, C., Girish, B.P., Reddy, S.P., 2014. Aflatoxin B1-induced reproductive toxicity in male rats: possible mechanism of action. Int. J. Toxicol. 33, 155–161. https://doi.org/10.1177/1091581814530764.
Torraca, V., Otto, N.A., Tavakoli-Tameh, A., Meijer, A.H., 2017. The inflammatory chemokine Cxcl18b exerts neutrophil-specific chemotaxis via the promiscuous chemokine receptor Cxcr2 in zebrafish. Dev. Comp. Immunol. 67, 57–65. https://doi.org/10.1016/j.dci.2016.10.014.
Troxel, C.M., Reddy, A.P., O'Neal, P.E., Hendricks, J.D., Bailey, G.S., 1997. In vivo aflatoxin B1 metabolism and hepatic DNA adduction in zebrafish (Danio rerio). Toxicol. Appl. Pharmacol. 143, 213–220. https://doi.org/10.1006/taap.1996.8058.
Turner, P.C., Collinson, A.C., Cheung, Y.B., Gong, Y., Hall, A.J., Prentice, A.M., Wild, C.P., 2007. Aflatoxin exposure in utero causes growth faltering in Gambian infants. Int. J. Epidemiol. 36, 1119–1125. https://doi.org/10.1093/ije/dym122.
Ugbaja, R.N., Okedairo, O.M., Oloyede, A.R., Ugwor, E.I., Akinloye, D.I., Ojo, O.P., Ademuyiwa, O., 2020. Probiotics consortium synergistically ameliorates aflatoxin B1-induced disruptions in lipid metabolism of female albino rats. Toxicon 186, 109–119. https://doi.org/10.1016/j.toxicon.2020.08.007.
van der Fels-Klerx, H.J., Burgers, S.L.G.E., Booij, C.J.H., 2010. Descriptive modelling to predict deoxynivalenol in winter wheat in the Netherlands. Food Addit. Contam. 27, 636–643. https://doi.org/10.1080/19440040903571762.
Veldman, M.B., Lin, S., 2008. Zebrafish as a developmental model organism for pediatric research. Pediatr. Res. 64, 470–476.

Wallace, K.N., Pack, M., 2003. Unique and conserved aspects of gut development in zebrafish. Dev. Biol. 255, 12–29. https://doi.org/10.1016/S0012-1606(02)00034-9.

Wang, J., Tang, L., Glenn, T.C., Wang, J.S., 2016. Aflatoxin B1 induced compositional changes in gut microbial communities of male F344 rats. Toxicol. Sci. 150, 54–63. https://doi.org/10.1093/toxsci/kfv259.

Wangikar, P.B., Dwivedi, P., Sinha, N., Sharma, A.K., Telang, A.G., 2005. Effects of aflatoxin B1 on embryo fetal development in rabbits. Food Chem. Toxicol. 43, 607–615. https://doi.org/10.1016/j.fct.2005.01.004.

Wild, C.P., Jiang, Y., Allen, S.J., Jansen, L.A.M., Hall, A.J., Montesano, R., 1990. Aflatoxin—albumin adducts in human sera from different regions of the world. Carcinogenesis 11, 2271–2274. https://doi.org/10.1093/carcin/11.12.2271.

Williams, C.H., Hong, C.C., 2011. Multi-step usage of in vivo models during rational drug design and discovery. Int. J. Mol. Sci. 12, 2262–2274. https://doi.org/10.3390/ijms12042262.

Wrighton, P.J., Oderberg, I.M., Goessling, W., 2019. There is something fishy about liver cancer: zebrafish models of hepatocellular carcinoma. Cell. Mol. Gastroenterol. Hepatol. 8, 347–363. https://doi.org/10.1016/j.jcmgh.2019.05.002.

Wu, T.S., Cheng, Y.C., Chen, P.J., Huang, Y.T., Yu, F.Y., Liu, B.H., 2019. Exposure to aflatoxin B1 interferes with locomotion and neural development in zebrafish embryos and larvae. Chemosphere 217, 905–913. https://doi.org/10.1016/j.chemosphere.2018.11.058.

Yang, X., Liu, L., Chen, J., Xiao, A., 2017. Response of intestinal bacterial flora to the long-term feeding of aflatoxin B1 (AFB1) in mice. Toxins 9, 317. https://doi.org/10.3390/toxins9100317.

Yu, Q., Huo, J., Zhang, Y., Liu, K., Cai, Y., Xiang, T., Jiang, Z., Zhang, L., 2020. Tamoxifen-induced hepatotoxicity via lipid accumulation and inflammation in zebrafish. Chemosphere 239, 124705. https://doi.org/10.1016/j.chemosphere.2019.124705.

Yu, J., Wu, F., Hennessy, D.A., 2018. The impact of climate change on aflatoxin contamination in US corn, in: Agricultural & Applied Economics Association Annual Meeting. Washington. https://doi.org/10.22004/ag.econ.273914.

Yuan, X., Song, M., Devine, P., Bruneau, B.G., Scott, I.C., Wilson, M.D., 2018. Heart enhancers with deeply conserved regulatory activity are established early in zebrafish development. Nat. Commun. 9, 1–14. https://doi.org/10.1038/s41467-018-07451-z.

Yunus, A.W., Ghareeb, K., Abd-El-Fattah, A.A.M., Twaruzek, M., Böhm, J., 2011. Gross intestinal adaptations in relation to broiler performance during chronic aflatoxin exposure. Poult. Sci. 90, 1683–1689. https://doi.org/10.3382/ps.2011-01448.

Zhang, L.Y., Zhan, D.L., Chen, Y.Y., Wang, W.H., He, C.Y., Lin, Y., Lin, Y.C., Lin, Z.N., 2019. Aflatoxin B1 enhances pyroptosis of hepatocytes and activation of Kupffer cells to promote liver inflammatory injury via dephosphorylation of cyclooxygenase-2: an in vitro, ex vivo and in vivo study. Arch. Toxicol. 93, 3305–3320. https://doi.org/10.1007/s00204-019-02572-w.